

# Vibrational Spectroscopy of the Electronically Excited State. 5. Time-Resolved Resonance Raman Study of Tris(bipyridine)ruthenium(II) and Related Complexes. Definitive Evidence for the "Localized" MLCT State

Paul G. Bradley, Nurit Kress, Boyce A. Hornberger, Richard F. Dallinger,\*<sup>1</sup> and William H. Woodruff\*

Contribution from the Department of Chemistry, University of Texas, Austin, Texas 78712.  
Received May 26, 1981

**Abstract:** Time-resolved resonance Raman (TR<sup>3</sup>) spectra of the emissive and photochemically active metal-to-ligand charge-transfer (MLCT) electronic states of Ru(bpy)<sub>3</sub><sup>2+</sup>, Os(bpy)<sub>3</sub><sup>2+</sup>, and related complexes are reported. These spectra are compared to those of complexes containing neutral bipyridine and bipyridine radical anion. In the Ru(bpy)<sub>3</sub><sup>2+</sup> complex it is conclusively demonstrated that the realistic formulation of the MLCT state is [Ru<sup>III</sup>(bpy)<sub>2</sub>(bpy<sup>-</sup>)]<sup>2+</sup>. This conclusion is reached by four lines of evidence: (i) large frequency shifts in bpy modes in the MLCT state, which approximate those observed upon one-electron chemical reduction of bpy to bpy<sup>-</sup>; (ii) the TR<sup>3</sup> spectrum observed upon saturation of the MLCT state, which exhibits peaks due to both neutral and radical-like bipyridine; (iii) precise frequencies of "unshifted" bpy modes in the MLCT state, which resemble Ru<sup>III</sup>(bpy)<sub>3</sub><sup>3+</sup>; and (iv) the frequency shifts observed in MLCT states of bis(bipyridine)ruthenium(II) complexes, which are essentially the same as those of the tris chelate. In Os(bpy)<sub>3</sub><sup>2+</sup>, criteria ii-iv above have not been successfully tested, but the magnitudes of the large excited state frequency shifts strongly suggest the formulation [Os<sup>III</sup>(bpy)<sub>2</sub>(bpy<sup>-</sup>)]<sup>2+</sup> for the MLCT state of this complex.

In a previous communication,<sup>2</sup> we reported the first direct observation of the vibrational spectrum of an electronically excited state of a metal complex in solution. The excited state observed was the emissive and photochemically active MLCT state of Ru(bpy)<sub>3</sub><sup>2+</sup>, the vibrational spectrum of which was acquired by time-resolved resonance Raman (TR<sup>3</sup>) spectroscopy. In this and other previous studies<sup>2,10-12</sup> we have demonstrated the enormous, virtually unique utility of TR<sup>3</sup> in structural elucidation of electronically excited states in solution.

The photochemical and photophysical properties of Ru(bpy)<sub>3</sub><sup>2+</sup> and related d<sup>6</sup> polypyridine complexes have been the subject of intense recent interest.<sup>3-9</sup> The interest in these complexes is due to their potential in photochemical energy conversion as well as their intrinsically significant excited state properties. The structures of the excited states of these complexes are clearly of great interest, and we now report an extended TR<sup>3</sup> study of these structures.

The TR<sup>3</sup> data presented in our original report<sup>2</sup> comprised the symmetric C-C and C-N stretching modes of bipyridine in the excited state of Ru(bpy)<sub>3</sub><sup>2+</sup>. We argued from the magnitudes of the frequency shifts in the bpy modes between the ground and excited states that the excited state MLCT electron density was localized on one ligand, rather than delocalized over all three, on the vibrational time scale. If this is the case, the MLCT excited state may be realistically formulated as Ru<sup>III</sup>(bpy)<sub>2</sub>(bpy<sup>-</sup>)<sup>2+</sup>, which

has maximum symmetry of C<sub>2</sub>, rather than the heretofore commonly presumed Ru<sup>III</sup>(bpy<sup>-1/3</sup>)<sub>3</sub><sup>2+</sup>, which may have D<sub>3</sub> symmetry. We shall refer to the former structure as the "localized" model of the excited state, and the latter as the "delocalized" model.

The localized model was suggested prior to our communication<sup>2</sup> on the basis of emission and excited state absorption data,<sup>6,7</sup> and since then our communication has been supported by luminescence depolarization investigations.<sup>8,9</sup> However, these lines of evidence lack structural specificity and/or direct applicability to solution conditions. EPR results on ligand-reduced Ru(bpy)<sub>3</sub><sup>+</sup> demonstrate that the localized model is valid for a ground-state Ru(II) species in solution.<sup>13</sup> In this work we present conclusive TR<sup>3</sup> evidence that the principal excited state Ru(bpy)<sub>3</sub><sup>2+</sup> structure present in solution within a maximum of 1 ns after excitation is the localized species. We present strong evidence that the excited states of Os(bpy)<sub>3</sub><sup>2+</sup> and Ru(bpy)<sub>2</sub>L<sub>2</sub><sup>2+</sup> (L = NH<sub>3</sub>, or 1/2 en, en = ethylenediamine) also conform to the localized model.

## Experimental Section

**Reagents.** Several sources of Ru(bpy)<sub>3</sub><sup>2+</sup> were employed in the present study, with complete reproducibility of results. Commercially available Ru(bpy)<sub>3</sub>Cl<sub>2</sub> was purchased from Alfa Inorganics and Strem Chemical Co. and used without further purification. This salt was also synthesized in these laboratories by two procedures. The initial step in both was isolation of impure Ru(bpy)<sub>3</sub>Cl<sub>2</sub> by refluxing RuCl<sub>3</sub> with stoichiometric amounts of bpy in dimethylformamide (DMF) and evaporating the resulting solution to dryness. In one procedure, the resulting solid was redissolved in ethanol, then purified by chromatography on a Sephadex LH-20 column. The solvent was subsequently stripped to obtain the purified solid. In the second procedure, the impure solid was passed down an anion exchange column which had been previously converted to the iodide form. The eluent thus was converted to Ru(bpy)<sub>3</sub>I<sub>2</sub>. This solution was evaporated to dryness, redissolved in a small volume of ethanol, and allowed to stand at -10 °C. Crystals of Ru(bpy)<sub>3</sub>I<sub>2</sub> were isolated. These were redissolved, ion exchanged for chloride, and evaporated to dryness to produce Ru(bpy)<sub>3</sub>Cl<sub>2</sub> (the chloride salt of Ru(bpy)<sub>3</sub><sup>2+</sup> does not crystallize satisfactorily; the iodide salt is somewhat unstable toward laser illumination). Finally, samples of Ru(bpy)<sub>3</sub>Cl<sub>2</sub> and Ru(bpy)<sub>3</sub>(ClO<sub>4</sub>)<sub>2</sub> were generously donated by Professor Allen J. Bard. Purity criteria were electronic absorption spectrophotometry<sup>14</sup> and emission spectroscopy (absence of impurities luminescing at shorter wavelengths than Ru-

(1) Correspondence for this author should be addressed to the Department of Chemistry, Purdue University, West Lafayette, Indiana 47907.

(2) Dallinger, R. F.; Woodruff, W. H. *J. Am. Chem. Soc.* **1979**, *101*, 1355.

(3) (a) Hager, G. D.; Crosby, G. A. *J. Am. Chem. Soc.* **1975**, *97*, 7031.

(b) Hager, G. D.; Watts, R. J.; Crosby, G. A. *Ibid.* **1975**, *97*, 7037. (c) Hipps, K. W.; Crosby, G. A. *Ibid.* **1975**, *97*, 7042. (d) Crosby, G. A.; Elfring, W. H., Jr. *J. Phys. Chem.* **1976**, *80*, 2206.

(4) Meyer, T. J. *Acc. Chem. Res.* **1978**, *11*, 94.

(5) Balzani, V.; Bolletta, F.; Gandolfi, M. T.; Maestri, M. *Top. Current Chem.* **1978**, *75*, 1.

(6) DeArmond, M. K. *Acc. Chem. Res.* **1974**, *7*, 309.

(7) Sutlin, N.; Creutz, C. *Adv. Chem. Ser.* **1978**, *No. 138*, 1-27.

(8) Hipps, K. W. *Inorg. Chem.* **1980**, *19*, 1390.

(9) Felix, F.; Ferguson, J.; Güdel, H. U.; Ludi, A. *J. Am. Chem. Soc.* **1980**, *102*, 4096.

(10) Dallinger, R. F.; Guanci, J. J. Jr.; Woodruff, W. H.; Rodgers, M. A. *J. Am. Chem. Soc.* **1979**, *101*, 1355.

(11) Dallinger, R. F.; Miskowski, V. M.; Gray, H. B.; Woodruff, W. H. *J. Am. Chem. Soc.* **1981**, *103*, 1595.

(12) Dallinger, R. F.; Farquharson, S.; Woodruff, W. H.; Rodgers, M. A. *J. Am. Chem. Soc.*, preceding paper in this issue.

(13) Motten, A. G.; Dearmond, M. K.; Hauck, K. W. *Chem. Phys. Lett.* **1981**, *79*, 541.

(14) Crosby, G. A.; Perkins, W. G.; Klassen, D. M. *J. Chem. Phys.* **1965**, *43*, 1498.

(bpy)<sub>3</sub><sup>2+</sup>). Resonance Raman and TR<sup>3</sup> results were independent of the source of the Ru(bpy)<sub>3</sub><sup>2+</sup> and of the identity of the anion (Cl<sup>-</sup>, I<sup>-</sup>, ClO<sub>4</sub><sup>-</sup>, SO<sub>4</sub><sup>2-</sup>, BF<sub>4</sub><sup>-</sup>).

For the Raman spectra the solid was dissolved in a deaerated solution (bubbling N<sub>2</sub>, 20 min) prepared from reagent grade Na<sub>2</sub>SO<sub>4</sub> and deionized water. The final concentration of sulfate was 0.5 M. The 984 cm<sup>-1</sup> (ν<sub>1</sub>) Raman mode of SO<sub>4</sub><sup>2-</sup> was used as an internal intensity reference in comparing the excited and ground state Raman spectra and for excitation wavelength comparisons. The final molar concentration of Ru(bpy)<sub>3</sub><sup>2+</sup> in solution was generally 3.5 × 10<sup>-4</sup> M. Whenever practicable, the identical solution was used for both the pulsed and the continuous wave Raman spectra.

The Os(bpy)<sub>3</sub>Cl<sub>2</sub> was prepared and purified by using the following procedure. OsCl<sub>4</sub>, purchased from Alpha Inorganics, and 2,2'-bipyridine in a molar ratio of 1:3.2 were dissolved in DMF and the solution was refluxed. After 3 days the characteristic dark green color of Os(bpy)<sub>3</sub><sup>2+</sup> was apparent and the reflux was discontinued. The solvent was removed by evaporation and the remaining green solid was dissolved in deionized water. This solution was washed three times with toluene to remove any excess organic substances. The water was then removed by slow evaporation, leaving a dark green solid. The solid was dissolved in a small volume of anhydrous ethanol. The Os(bpy)<sub>3</sub>Cl<sub>2</sub> was then purified by passing the solution down a column filled with Sephadex LH-20, eluting with absolute ethanol. The purified complex was obtained by collecting only the dark green band. Further purification was obtained by a second run down a fresh Sephadex column, collecting only the center of the dark green band.

The ethanol was removed by evaporation. The resulting green solid was dissolved in deionized water and subjected to the spectrophotometric purity criteria. The absorption spectra were identical with those previously reported in the literature.<sup>15,16</sup> For the Raman spectra, the concentration of the Os(bpy)<sub>3</sub><sup>2+</sup> in deionized water was 4.2 × 10<sup>-4</sup> M and the concentration of Na<sub>2</sub>SO<sub>4</sub>, the internal intensity standard, was 0.5 M. The same solution was used to obtain both the TR<sup>3</sup> and continuous wave Raman spectra.

Ru(bpy)<sub>2</sub>(NH<sub>3</sub>)<sub>2</sub><sup>2+</sup> was prepared and purified by using a modification of the procedures of Meyer et al.<sup>17</sup> and Dwyer et al.<sup>18</sup> RuCl<sub>3</sub> was mixed with 2,2'-bipyridine in a molar ratio of 1:2 and was dissolved in DMF. This solution was refluxed for about 8 h, after which acetone was added to the solution and a solid was obtained (impure Ru(bpy)<sub>2</sub>Cl<sub>2</sub>). The dried solid was then dissolved in aqueous ammonium hydroxide. [Ru(bpy)<sub>2</sub>(NH<sub>3</sub>)<sub>2</sub>]Cl<sub>2</sub> was precipitated from this solution upon addition of sodium chloride. Further purification was obtained by dissolving the dried solid in anhydrous ethanol and eluting this solution down a column packed with Sephadex LH-20. The reddish-orange band was collected and the solvent was removed by evaporation. An analogous procedure which uses ethylenediamine in stoichiometric amounts was employed to prepare [Ru(bpy)<sub>2</sub>(en)]<sup>2+</sup>.

Recrystallization of [Ru(bpy)<sub>2</sub>(NH<sub>3</sub>)<sub>2</sub>]<sup>2+</sup> or [Ru(bpy)<sub>2</sub>(en)]<sup>2+</sup> with either Cl<sup>-</sup> or I<sup>-</sup> as a counterion was difficult, and an alternative purification scheme which uses different counterions was employed. Precipitation from the aqueous ammonia or ethylenediamine solution with NaBF<sub>4</sub> and subsequent recrystallization proved simple, and chromatography was not necessary.

The UV-vis absorption spectrum obtained from the product dissolved in deionized water agreed with previously published spectra of [Ru(bpy)<sub>2</sub>(L)<sub>2</sub>]<sup>2+</sup>.<sup>19</sup> For the Raman spectra reported in this paper, the molar concentration of Ru(bpy)<sub>2</sub>(L)<sub>2</sub><sup>2+</sup> was ca. 1 × 10<sup>-3</sup> M. The same solutions were used to obtain both the TR<sup>3</sup> and the continuous Raman spectra.

**Instrumental.** Both visible and ultraviolet excitation sources were used in obtaining the continuous wave Raman spectra of these three complexes. The visible excitation sources were the 496.5, 488.0, or 457.9 nm lines of the Ar<sup>+</sup> continuous wave laser. Typical laser powers were 50–150 mW at the sample. The ultraviolet excitation sources were either the 363.8 or 351.1 nm lines of the Ar<sup>+</sup> continuous wave laser or the 356.4 or 350.7 nm line of the Kr<sup>+</sup> continuous wave laser. Typical laser power was about 65 mW at the sample. A SPEX Ramalog EU spectrometer was used to disperse and scan the Raman scattered radiation. The scattered light was detected with a thermoelectrically cooled RCA C31034A photomultiplier. The resulting signal was processed by an ORTEC 9300 series photon counter and converted to an analog signal for strip chart recording.

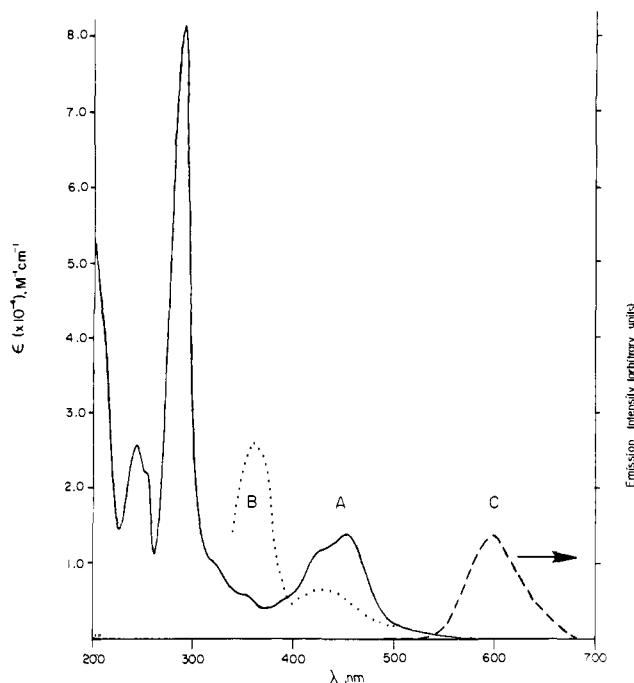


**Figure 1.** Absorption and emission<sup>20</sup> spectra of Ru(bpy)<sub>3</sub><sup>2+</sup> and the excited state transient absorption spectrum<sup>21</sup> of Ru(bpy)<sub>3</sub><sup>2+</sup>: (A) absorption spectrum of Ru(bpy)<sub>3</sub><sup>2+</sup>; (B) absorption spectrum of \*Ru(bpy)<sub>3</sub><sup>2+</sup>; (C) emission spectrum. Conditions: room temperature, aqueous solution.

The TR<sup>3</sup> instrumental setup used the harmonics of a pulsed Nd:YAG laser (Quanta-Ray DCR-1A) or a Nd:YAG pumped dye laser (Quanta-Ray PDL-1) as sources both to create the excited states and to effect the Raman scattering. The second (531.8 nm) and third (354.5 nm) harmonics of the Nd:YAG laser were employed, as was a 440 nm line from the dye laser (using Coumarin 440 dye). Except in the 440 nm experiments, the third harmonic was generally used as the probe wavelength for the Ru(bpy)<sub>3</sub><sup>2+</sup> excited state. Because of longer wavelength luminescence, the second harmonic could be utilized to observe the Os(bpy)<sub>3</sub><sup>2+</sup> excited state. Pulse characteristics were: pulse widths, 7 ns (Nd:YAG) or 5 ns (dye); per-pulse energy, of 1–5 mJ/pulse; repetition rate 10 Hz.

The same SPEX monochromator that was used in the continuous wave Raman experiments was used to disperse the Raman scattered light in the time-resolved experiment. In one signal amplification scheme, the photomultiplier output was amplified with a conventional electrometer and passed through first an on-off gate of ca. 1 μs temporal width and subsequently a lock-in amplifier, both of which were triggered by the 10 Hz repetition rate of the pulsed Nd:YAG laser, to reject spurious photomultiplier noise. In later experiments, a PAR Model 162 boxcar averager with Model 165 gated integrators was used to perform the same signal integration/noise rejection functions. Absorption spectra were obtained with a Cary 14 or Cary 210 spectrophotometer, and fluorescence spectra were obtained with a Varian UFS-330 or SPEX Fluorolog spectrofluorometer.

## Results

The electronic absorption and emission spectra of the ground state and MLCT excited state of Ru(bpy)<sub>3</sub><sup>2+</sup> are shown in Figure 1. It can be seen that the ground state absorption at the wavelength of the Nd:YAG third harmonic, 354.5 nm, is considerable. Therefore, laser pulses at this wavelength are suitable for generating good yields of the MLCT excited state. It is also evident that the resonance condition for enhancement of Raman scattering in the MLCT excited state should be very favorable if 354.5 nm excitation is used, because this wavelength is virtually on top of the excited state absorption maximum at ca. 360 nm. Finally, the onset of the emission of the MLCT state occurs at long enough wavelengths so that Raman scattering produced by 354.5 nm excitation encounters no interference from the intrinsic luminescence of the complex. The same qualitative conditions are effective in the absorption and emission spectra of Os(bpy)<sub>3</sub><sup>2+</sup> except that the emission spectrum is at longer wavelength and

(15) Crosby, G. A.; Klassen, D. M.; Sabath, S. L. *Mol. Crystallogr.* **1966**, *1*, 453.

(16) Fergusson, J. E.; Harris, G. M. *J. Chem. Soc. A* **1966**, 1293.

(17) Sullivan, B. P.; Salmon, D. J.; Meyer, T. J. *Inorg. Chem.* **1978**, *17*, 3334.

(18) Dwyer, F. P.; Goodwin, H. A.; Gyarfás, E. C. *Aust. J. Chem.* **1963**, *16*, 544.

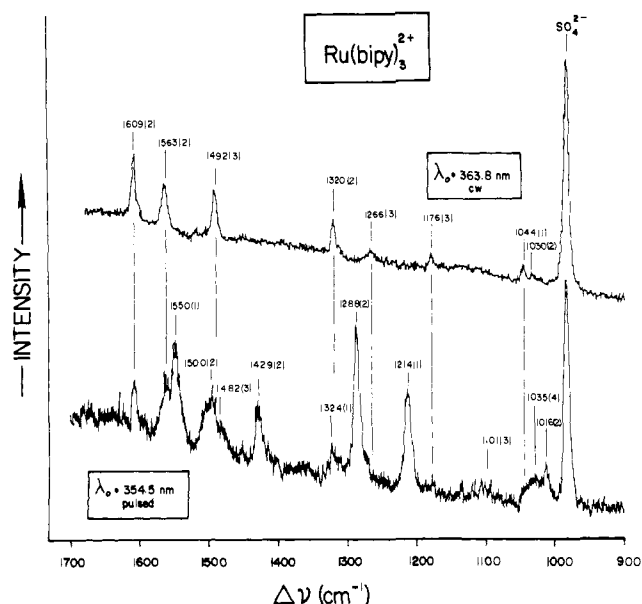


**Figure 2.** Upper trace: ground state (continuous wave excited) resonance Raman spectrum of  $\text{Ru}(\text{bpy})_3^{2+}$ . Lower trace:  $\text{TR}^3$  spectrum of the MLCT state,  $^*\text{Ru}(\text{bpy})_3^{2+}$ . The peaks at  $984\text{ cm}^{-1}$  are due to  $0.50\text{ M SO}_4^{2-}$  added as an internal intensity reference. The numbers in parentheses are standard deviations.

the quantum yield for luminescence is smaller than in the ruthenium complex.

The excited state  $\text{TR}^3$  results are obtained by illuminating the sample at an appropriate wavelength with a laser pulse of 5–7 ns duration. The laser pulse contains greater than tenfold excess of photons over molecules in the illuminated volume of solution (a cylinder approximately 1 mm in diameter and 1 mm in depth). The excited state lifetimes, ca. 600 ns for  $\text{Ru}(\text{bpy})_3^{2+}$ ,<sup>3</sup> 20 ns for  $\text{Os}(\text{bpy})_3^{2+}$ ,<sup>3</sup> and 10 ns for  $[\text{Ru}(\text{bpy})_2(\text{NH}_3)_2]^{2+}$ , are comparable to or longer than the laser pulse width. Therefore, the adsorbed photons from the laser pulse produce an appreciable concentration of excited states (in the case of  $\text{Ru}(\text{bpy})_3^{2+}$ , essentially complete saturation can be achieved). Other photons from the same laser pulse are Raman scattered by the sample, both by the ground state and excited state complexes. The dominant spectrum which is observed depends upon the proportion of excited state to ground state concentration averaged over the entire laser pulse (average degree of saturation) and the degree of resonance enhancement of the Raman scattering of each of the electronic states.

All of the systems reported here were investigated by  $\text{TR}^3$  as described above, using pulsed illumination at 354.5 nm. Complementary ground state (continuous wave illumination) studies were performed with use of the 363.8 or 351.1 nm lines of the  $\text{Ar}^+$  laser and/or the 356.4 or 350.7 nm lines of the  $\text{Kr}^+$  laser. In addition, the  $\text{Ru}(\text{bpy})_3^{2+}$  system was examined by  $\text{TR}^3$  with 440 nm illumination (Nd:YAG pumped dye laser, Coumarin 440) and complementary continuous wave study at 457.9 nm ( $\text{Ar}^+$  laser), and the  $\text{Os}(\text{bpy})_3^{2+}$  system was examined by  $\text{TR}^3$  with 531.8 nm illumination (Nd:YAG second harmonic) and complementary continuous wave study at 530.9 nm ( $\text{Kr}^+$  laser).

The continuous wave and  $\text{TR}^3$  spectra of  $\text{Ru}(\text{bpy})_3^{2+}$  in the frequency region of the C–C and C–N stretches ( $900\text{--}1700\text{ cm}^{-1}$ ), obtained with use of near-UV excitation, are compared in Figure 2. The  $\text{TR}^3$  spectrum obtained with improved signal-to-noise ratio, including the low-frequency region of the spectrum, is shown in Figure 3. The peak at  $984\text{ cm}^{-1}$  in Figure 2 is the internal intensity reference, the symmetric stretching vibration of  $\text{SO}_4^{2-}$  ( $0.50\text{ M Na}_2\text{SO}_4$  added). The continuous wave and  $\text{TR}^3$  spectra were obtained on the identical sample, using a Shriver rotating cell<sup>22</sup> and  $135^\circ$  backscattering illumination geometry. All of the

**Table I.** Ground State Resonance Raman Frequencies [ $\text{cm}^{-1}$  ( $\pm\sigma$ )] of  $\text{Ru}^{\text{III}}(\text{bpy})_3^{3+}$  and  $\text{Ru}^{\text{II}}(\text{bpy})_3^{2+}$  Compared to "Unshifted" Frequencies in the MLCT State ( $^*\text{Ru}(\text{bpy})_3^{2+}$ ) of  $\text{Ru}^{\text{II}}(\text{bpy})_3^{2+}$

$\text{Ru}^{\text{II}}(\text{bpy})_3^{2+}$ $\lambda_0 = 457.9\text{ nm}$	$\text{Ru}^{\text{III}}(\text{bpy})_3^{3+}$ $\lambda_0 = 457.9,$ $647.1\text{ nm}$	"unshifted" peaks <sup>a</sup> of $^*\text{Ru}(\text{bpy})_3^{2+}$
1030 (2)		
1044 (1) <sup>b</sup>		1044
	1112	1101 (3)
1176 (3)	1178	1175 (2)
1266 (3) <sup>b</sup>		
1276 (2)	1280 (3)	
1320 (2)	1326 (2)	1324 (1)
1492 (3)	1499 (3)	1500 (2)/1482 (3) <sup>c</sup>
1563 (2)	1566 (3)	1566 (2)
1609 (2)	1608 (2)	1609 (1)

<sup>a</sup> Peaks due to "neutral bpy" in the MLCT state. See text.

<sup>b</sup> Frequencies noted with near-UV excitation (bpy  $\pi \rightarrow \pi^*$  resonance). <sup>c</sup> See text for discussion of the frequency correlation of these modes.

Raman peaks having sufficient intensity to allow measurement of depolarization ratios are polarized ( $\rho \sim 0.3\text{--}0.5$ ) in both the continuous wave and  $\text{TR}^3$  spectra.

The ground state spectrum in Figure 2 exhibits the typical features of the Raman spectrum of a bipyridine complex.<sup>2,23,24</sup> Seven relatively intense peaks dominate the spectrum. These may be approximately described as the seven symmetric C–C and C–N stretches expected of bipyridine in any point group wherein the two pyridine rings are related by a symmetry element. This simple assignment must, however, be viewed with a certain amount of caution. Bipyridine also possesses four symmetric in-plane C–H wags which are expected in the same frequency region and which may mix with the bpy stretches to produce more than seven Raman-active modes with appreciable intensity. Evidence that this occurs may be seen by comparing the ground-state spectrum of  $\text{Ru}(\text{bpy})_3^{2+}$  obtained by using 457.9 nm excitation<sup>2</sup> to that in Figure 2. It is seen that the peaks at 1028 and  $1276\text{ cm}^{-1}$  (457.9 nm) disappear or are greatly reduced in intensity in Figure 2. Furthermore, the ground-state spectrum in Figure 2 exhibits peaks at 1044 and  $1266\text{ cm}^{-1}$  which were absent with 457.9 nm excitation. Nevertheless, the bipyridine modes in this frequency region which have large intensity in near-UV  $\pi \rightarrow \pi^*$  resonance (see Figure 1; 457.9 nm excitation represents direct MLCT resonance) are expected to be predominantly the C–C and C–N stretches. The details of the resonance Raman spectroscopy of  $\text{M}(\text{bpy})_3^{n+}$  complexes are discussed elsewhere.<sup>23</sup>

Because the oxidation state of the metal ion in the MLCT state of  $\text{Ru}(\text{bpy})_3^{2+}$  may be approximately characterized as  $\text{Ru}(\text{III})$ ,<sup>3</sup> we have examined the RR spectrum of the ground state of the corresponding trivalent ruthenium complex,  $\text{Ru}(\text{bpy})_3^{3+}$ . A comparison of the  $\text{Ru}(\text{bpy})_3^{2+}$  and  $\text{Ru}(\text{bpy})_3^{3+}$  frequencies in the  $1000\text{--}1700\text{ cm}^{-1}$  region is given in Table I, with certain frequencies of the MLCT state of  $\text{Ru}(\text{bpy})_3^{2+}$  included.

The  $\text{TR}^3$  spectra of the MLCT state comprising the predominant fraction of excited  $\text{Ru}(\text{bpy})_3^{2+}$  species averaged over the time scale of our laser excitation pulse (7 ns) are shown in Figures 2 and 3. The predominant MLCT species has been variously denoted "Triplet charge-transfer ( $^3\text{CT}$ )",<sup>5</sup> " $d\pi^*$ ",<sup>3</sup> or simply  $^*\text{Ru}(\text{bpy})_3^{2+}$ .<sup>4</sup> We adopt the latter nomenclature. The excited state species initially produced by the adsorption of a photon is the "singlet charge-transfer" state. However, due to extremely fast "intersystem crossing" and internal conversion processes, the lifetime of the  $^1\text{CT}$  state is  $\leq 10\text{ ps}$ <sup>25</sup> and therefore this state is

(21) Creutz, C.; Chou, M.; Netzel, T. L.; Okumura, M.; Sutin, N. *J. Am. Chem. Soc.* **1980**, *102*, 1309.

(22) Shriver, D. F.; Dunn, J. B. R. *Appl. Spectrosc.* **1974**, *28*, 319.

(23) Clark, R. J. H.; Turtle, P. C.; Strommen, D. P.; Streusand, B.; Kincaid, J.; Nakamoto, K. *Inorg. Chem.* **1977**, *16*, 84.

(24) Chisholm, M. H.; Huffman, J. C.; Rothwell, I. P.; Bradley, P. G.; Kress, N.; Woodruff, W. H. *J. Am. Chem. Soc.* **1981**, *103*, 4945.

(19) Bryant, G. M.; Fergusson, J. E.; Powell, H. K. *J. Aust. J. Chem.* **1971**, *24*, 257.

(20) Crosby, G. A. *Acc. Chem. Res.* **1975**, *8*, 231.

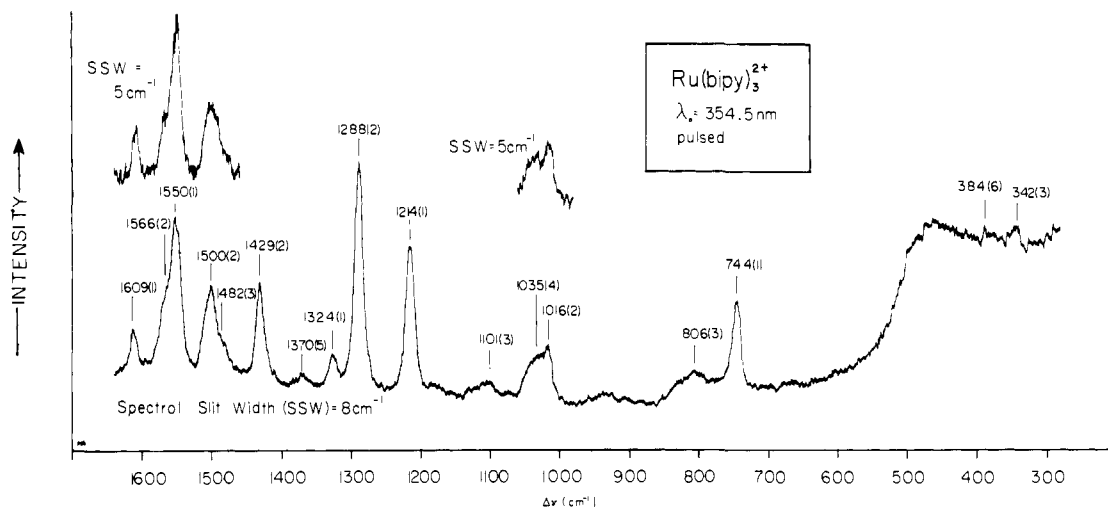


Figure 3. TR<sup>3</sup> spectrum of \*Ru(bpy)<sub>3</sub><sup>2+</sup> including the low-frequency region (300–1000 cm<sup>-1</sup>). The numbers in parentheses are standard deviations.

Table II. Ground state (Continuous-Wave-Excited) and Pulse-Excited Resonance Raman Frequencies (cm<sup>-1</sup>) of *cis*-[Ru(bpy)<sub>2</sub>(en)]<sup>2+</sup>,<sup>a</sup> Compared to Shifted Frequencies in the MLCT State of Ru(bpy)<sub>3</sub><sup>2+</sup>

ground state λ <sub>0</sub> = 356.4 nm	pulse excited λ <sub>0</sub> = 354.5 nm	shifted peaks <sup>b</sup> of *Ru(bpy) <sub>3</sub> <sup>2+</sup>
	1015 <sup>d</sup>	1016
	1031 <sup>d</sup>	1035
1037	1041	
1174	1176	
	1217 <sup>d</sup>	1214
1275	1272	
	1288 <sup>d</sup>	1288
1321	1318	
	1430 <sup>d</sup>	1429
1450	1448	
1490	1506/1498 <sup>c,d</sup>	1500/1482 <sup>c</sup>
	1554	1550
1562	1564	
1606	1607	

<sup>a</sup> Similar results were obtained for *cis*-[Ru(bpy)<sub>2</sub>(NH<sub>3</sub>)<sub>2</sub>]<sup>2+</sup>, which however may photoaquate ammonia ligands or photoisomerize to trans upon laser irradiation. <sup>b</sup> Peaks due to "bpy<sup>-</sup>" in the MLCT state. <sup>c</sup> See text for discussion of the frequency correlation of these modes. <sup>d</sup> Excited state peaks of [Ru(bpy)<sub>2</sub>(en)]<sup>2+</sup>.

not observed in our TR<sup>3</sup> spectra. The MLCT state which is responsible for the TR<sup>3</sup> spectra in Figures 2 and 3 is \*Ru(bpy)<sub>3</sub><sup>2+</sup>, the emissive and photochemically active state which has a lifetime of ca. 600 ns (room temperature, aqueous solution). Luminescence intensity measurements as a function of laser pulse energy show that the \*Ru(bpy)<sub>3</sub><sup>2+</sup> state is ca. 90% saturated under the TR<sup>3</sup> illumination conditions in both Figures 2 and 3. In these multilevel systems, 100% saturation is taken to imply 100% conversion to the excited state.<sup>3-5</sup>

Table II presents ground state and TR<sup>3</sup> frequencies for [Ru(bpy)<sub>2</sub>(en)]<sup>2+</sup>. The data for *cis*-[Ru(bpy)<sub>2</sub>(NH<sub>3</sub>)<sub>2</sub>]<sup>2+</sup> are similar. In the pulse-excited spectra of these complex peaks are observed due both to the ground state and the MLCT excited state, because the excited state lifetime is reduced to ca. 10 ns. Therefore, the excited state cannot be saturated by our 7 ns laser pulses at any reasonable per-pulse energy. The ammine system is complicated by possible photoisomerization and photoaquation of the NH<sub>3</sub> ligands. Nevertheless, the frequency shifts of the observed bipyridine modes in the MLCT state of this complex are qualitatively the same as those observed in \*Ru(bpy)<sub>3</sub><sup>2+</sup>. Photoisomerization is not possible for [Ru(bpy)<sub>2</sub>(en)]<sup>2+</sup>, and no significant photoaquation was observed.

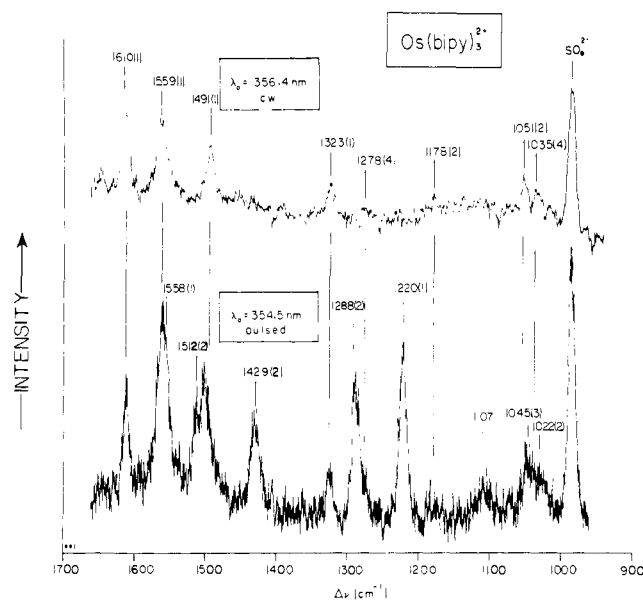


Figure 4. Upper trace: ground state (continuous wave excited) resonance Raman spectrum of Os(bpy)<sub>3</sub><sup>2+</sup>. Lower trace: TR<sup>3</sup> spectrum of the MLCT state, \*Os(bpy)<sub>3</sub><sup>2+</sup>. The peaks at 984 cm<sup>-1</sup> are due to 0.50 M SO<sub>4</sub><sup>2-</sup> added as an internal intensity reference. The numbers in parentheses are standard deviations.

The ground state and TR<sup>3</sup> spectra of Os(bpy)<sub>3</sub><sup>2+</sup> are shown in Figure 4, and the TR<sup>3</sup> spectra of Ru(bpy)<sub>3</sub><sup>2+</sup> and Os(bpy)<sub>3</sub><sup>2+</sup> are compared in Figure 5. The excited state lifetime of Os(bpy)<sub>3</sub><sup>2+</sup> is ca. 20 ns (room temperature, aqueous solution)<sup>3</sup> and therefore the TR<sup>3</sup> spectra of this complex in Figures 4 and 5 exhibit peaks due to ground state Os(bpy)<sub>3</sub><sup>2+</sup> as well as \*Os(bpy)<sub>3</sub><sup>2+</sup>, because the saturation condition obtained in the TR<sup>3</sup> spectra of \*Ru(bpy)<sub>3</sub><sup>2+</sup> is lacking.

In a companion investigation to the present work, we have extensively studied the resonance Raman spectra of bipyridine radical anion (bpy<sup>-</sup>) prepared by alkali metal reduction of bpy.<sup>26</sup> The radical has been shown to exist in solution as the alkali metal complex and to lack a center of inversion,<sup>26</sup> therefore it is probably the N-bonded bidentate chelate M<sup>+</sup>(bpy<sup>-</sup>). Details of this study will be discussed elsewhere.<sup>27</sup> The RR spectrum of Li<sup>+</sup>(bpy<sup>-</sup>) is shown in Figure 6 and compared to the shifted peaks in the TR<sup>3</sup> spectrum of \*Ru(bpy)<sub>3</sub><sup>2+</sup>. The typical seven-peak pattern of the bpy structure is observed for Li<sup>+</sup>(bpy<sup>-</sup>), with an additional bpy<sup>-</sup>.

(26) Hornberger, B. A., M.S. Thesis, The University of Texas at Austin, 1980.

(27) Woodruff, W. H.; Hornberger, B. A., manuscript in preparation.

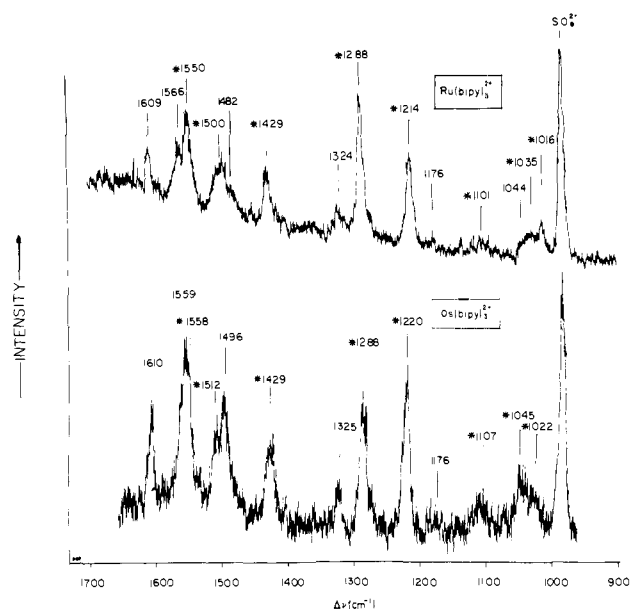


Figure 5. Comparison of the TR<sup>3</sup> spectra of \*Ru(bpy)<sub>3</sub><sup>2+</sup> (upper trace) and \*Os(bpy)<sub>3</sub><sup>2+</sup> (lower trace).

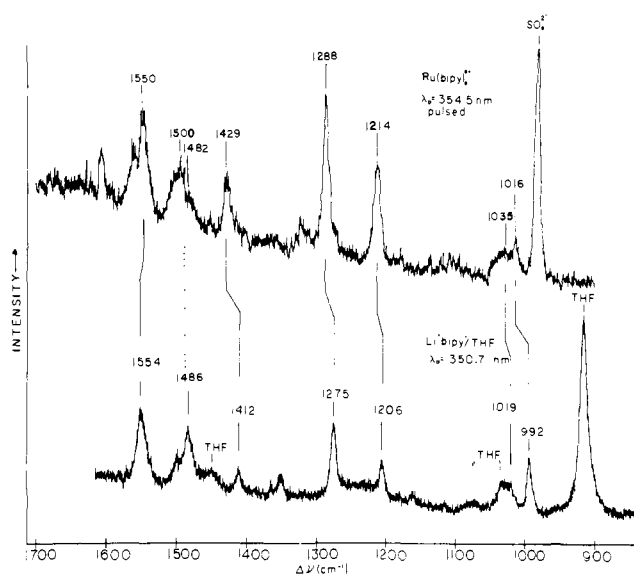


Figure 6. Comparison of the TR<sup>3</sup> spectrum of \*Ru(bpy)<sub>3</sub><sup>2+</sup> (upper trace) to the continuous wave excited spectrum of bipyridine radical anion (present as Li<sup>+</sup>(bpy<sup>·-</sup>)) (lower trace). The peaks marked as THF in the Li<sup>+</sup>(bpy<sup>·-</sup>) spectrum are due to the solvent, tetrahydrofuran. The peaks at 1160 and 1500 cm<sup>-1</sup> in the Li<sup>+</sup>(bpy<sup>·-</sup>) spectrum are due to an unidentified impurity.

peak at 1351 cm<sup>-1</sup>. The peaks at 1500 and 1160 cm<sup>-1</sup> are not due to bpy<sup>·-</sup>, but instead to a minor impurity of uncertain identity.<sup>26,27</sup>

### Discussion

The TR<sup>3</sup> evidence on \*Ru(bpy)<sub>3</sub><sup>2+</sup> is definitive in its support of the localized model for the principal MLCT species present within <1–7 ns after excitation. The structure of the \*Ru(bpy)<sub>3</sub><sup>2+</sup> species observed by TR<sup>3</sup> is essentially Ru<sup>III</sup>(bpy)<sub>2</sub>(bpy<sup>·-</sup>)<sup>2+</sup>. The maximum symmetry of this species is C<sub>2</sub>, although the actual symmetry could be lower if, for example, a nitrogen atom of one of the ligands were not coordinated to the metal ion. The TR<sup>3</sup> evidence on \*Os(bpy)<sub>3</sub><sup>2+</sup> and \*Ru(bpy)<sub>2</sub>(L)<sub>2</sub><sup>2+</sup>, while less than definitive, overwhelmingly favors a localized structure for the MLCT states of these complexes as well. In the case of \*Ru(bpy)<sub>3</sub><sup>2+</sup>, this conclusion is based upon four criteria, discussed below: the frequency shifts in \*Ru(bpy)<sub>3</sub><sup>2+</sup> compared to bpy<sup>·-</sup>; the TR<sup>3</sup> intensities in \*Ru(bpy)<sub>3</sub><sup>2+</sup> observed under substantially

saturated illumination conditions; the “unshifted” \*Ru(bpy)<sub>3</sub><sup>2+</sup> frequencies compared to ground state Ru(bpy)<sub>3</sub><sup>3+</sup>; and the frequency shifts observed in \*Ru(bpy)<sub>2</sub>(L)<sub>2</sub><sup>2+</sup>. In the Os(bpy)<sub>3</sub><sup>2+</sup> and Ru(bpy)<sub>2</sub>(L)<sub>2</sub><sup>2+</sup> systems, the excited state structures are deduced solely from frequency shift comparisons to bpy<sup>·-</sup>.

The TR<sup>3</sup> spectra of \*Ru(bpy)<sub>3</sub><sup>2+</sup> (Figures 2 and 3) consist essentially of two overlapping patterns of seven peaks in the 1000–1700 cm<sup>-1</sup> region, each comprising the seven symmetric C–C and C–N stretches of a bpy species (the weak features at 1370 and 1101 cm<sup>-1</sup> are overlooked for the present). The MLCT state is approximately 90% saturated by the intense laser pulses having short duration compared to the excited state lifetime, therefore none of the peaks in the TR<sup>3</sup> spectra of \*Ru(bpy)<sub>3</sub><sup>2+</sup> are due to residual ground state molecules. This can be seen by comparing the intensities of the 1609 cm<sup>-1</sup> “ground state” peak between the continuous wave and TR<sup>3</sup> spectra in Figure 2. Despite ~90% depletion of the ground state in the TR<sup>3</sup> spectrum, the 1609 cm<sup>-1</sup> peak retains approximately two thirds of its intensity. Apparently two sets of bpy frequencies are being observed in \*Ru(bpy)<sub>3</sub><sup>2+</sup>, one set at approximately the ground state frequencies and another set at considerably lower frequencies. This observation alone allows rejection of the possibility of D<sub>3</sub> symmetry for \*Ru(bpy)<sub>3</sub><sup>2+</sup>.

If the “localized” formulation of the structure of \*Ru(bpy)<sub>3</sub><sup>2+</sup> as Ru<sup>III</sup>(bpy)<sub>2</sub>(bpy<sup>·-</sup>)<sup>2+</sup> is realistic, the resonance Raman spectrum of \*Ru(bpy)<sub>3</sub><sup>2+</sup> can be predicted. A set of seven prominent symmetric modes should be observed at approximately the frequencies seen in Ru(III)(bpy)<sub>3</sub><sup>3+</sup>, with approximately two thirds the intensity of the ground state bpy modes (assuming similar excitation wavelengths and dominant bpy π → π\* resonance in both the continuous wave and TR<sup>3</sup> cases). The intensity of the localized 1609 cm<sup>-1</sup> peak fits this prediction, as noted above. The frequencies observed in \*Ru(bpy)<sub>3</sub><sup>2+</sup> fit this prediction as well, because close inspection of the seven “unshifted” peaks in the TR<sup>3</sup> spectrum reveals two significant frequency differences compared to ground state Ru(bpy)<sub>3</sub><sup>2+</sup>. The 1492 cm<sup>-1</sup> ground state peak is missing in the TR<sup>3</sup> spectrum; instead, two \*Ru(bpy)<sub>3</sub><sup>2+</sup> peaks appear near 1492 cm<sup>-1</sup>, one at 1500 cm<sup>-1</sup> and one at 1482 cm<sup>-1</sup>. Secondly, the 1320 cm<sup>-1</sup> ground state peak shifts to 1324 cm<sup>-1</sup> in \*Ru(bpy)<sub>3</sub><sup>2+</sup>. By comparison, Table I reveals that two significant frequency shifts occur upon oxidation of Ru(bpy)<sub>3</sub><sup>2+</sup> to Ru<sup>III</sup>(bpy)<sub>3</sub><sup>3+</sup>; the 1492 cm<sup>-1</sup> peak shifts to 1499 cm<sup>-1</sup>, and the 1320 cm<sup>-1</sup> peak shifts to 1326 cm<sup>-1</sup>, very closely mimicking the small shifts in the \*Ru(bpy)<sub>3</sub><sup>3+</sup> spectrum (if the 1492 cm<sup>-1</sup> ground state peak is regarded as correlated with the 1500 cm<sup>-1</sup> \*Ru(bpy)<sub>3</sub><sup>2+</sup> peak). In addition, a new feature appears in the spectrum of Ru<sup>III</sup>(bpy)<sub>3</sub><sup>3+</sup> at 1112 cm<sup>-1</sup>, close to the frequency of the weak peak at 1101 cm<sup>-1</sup> in the \*Ru(bpy)<sub>3</sub><sup>2+</sup> spectrum.

The localized formulation of \*Ru(bpy)<sub>3</sub><sup>2+</sup> predicts a second set of seven prominent Raman modes at frequencies approximating those of bpy<sup>·-</sup>. Figure 6 shows that this prediction is correct. The seven \*Ru(bpy)<sub>3</sub><sup>2+</sup> peaks which show substantial (average ~60 cm<sup>-1</sup>) shifts from the ground state frequencies may be correlated one-for-one with peaks of Li<sup>+</sup>(bpy<sup>·-</sup>) with an average deviation of 10 cm<sup>-1</sup>. In addition, the weak 1370 cm<sup>-1</sup> mode in \*Ru(bpy)<sub>3</sub><sup>2+</sup> is correlated with a bpy<sup>·-</sup> mode at 1351 cm<sup>-1</sup>. It is somewhat uncertain whether the 1486 cm<sup>-1</sup> bpy<sup>·-</sup> mode should be correlated with the \*Ru(bpy)<sub>3</sub><sup>2+</sup> mode at 1500 or 1482 cm<sup>-1</sup>, although the Ru<sup>III</sup>(bpy)<sub>3</sub><sup>3+</sup> evidence cited above suggests that the 1486/1482 cm<sup>-1</sup> correlation is appropriate. In the low-frequency region (<1000 cm<sup>-1</sup>, Figure 3) \*Ru(bpy)<sub>3</sub><sup>2+</sup> exhibits a prominent peak at 744 cm<sup>-1</sup> compared to 744 cm<sup>-1</sup> for Li<sup>+</sup>(bpy<sup>·-</sup>) and 672 cm<sup>-1</sup> for ground state Ru(bpy)<sub>3</sub><sup>2+</sup>. Weak features appear in the \*Ru(bpy)<sub>3</sub><sup>2+</sup> spectrum at 384 and 340 cm<sup>-1</sup>, compared to 375 cm<sup>-1</sup> (Ru(bpy)<sub>3</sub><sup>2+</sup>) and 308 cm<sup>-1</sup> (Li<sup>+</sup>(bpy<sup>·-</sup>)).

A final piece of evidence for the localized structure of \*Ru(bpy)<sub>3</sub><sup>2+</sup> is seen in the TR<sup>3</sup> spectrum of the MLCT state of *cis*-Ru(bpy)<sub>2</sub>(en)<sup>2+</sup>. If both \*Ru(bpy)<sub>3</sub><sup>2+</sup> and \*Ru(bpy)<sub>2</sub>(en)<sup>2+</sup> are delocalized MLCT states, then the frequency shifts in the bpy modes of the bis chelate upon MLCT excitation must be larger than those of the tris chelate. This is the case because, in the delocalized model of the MLCT state, the π\* orbitals of the bis chelate contain an average electron density of *e*/2 per bpy whereas

in the tris chelate the  $\pi^*$  electron density is only  $e^-/3$ . In the localized model, however, the frequency shifts in the bis and tris chelates should be the same, because the large shifts observed upon excitation in each case are due to production of the  $\text{Ru}^{\text{III}}(\text{bpy}^-)^{2+}$  moiety. Table II clearly shows that for every observable peak the shifts are similar for  $^*\text{Ru}(\text{bpy})_3^{2+}$  and  $^*\text{Ru}(\text{bpy})_2(\text{en})^{2+}$ .

Both  $\text{Os}(\text{bpy})_3^{2+}$  (Figure 4) and  $\text{Ru}(\text{bpy})_2(\text{en})^{2+}$  (Table II) exhibit frequency shifts in their bpy modes upon formation of their MLCT states which strongly support the formulation of the states as, respectively,  $\text{Os}^{\text{III}}(\text{bpy})_2(\text{bpy}^-)^{2+}$  and  $\text{Ru}^{\text{III}}(\text{bpy})(\text{bpy}^-)(\text{en})^{2+}$ . Due to the short excited state lifetimes of these complexes (20 and ca. 10 ns, respectively) it is not possible to achieve saturation of the excited states with reasonable laser pulse energies. Therefore, the definitive criteria for excited state structure based upon observation of both  $\text{M}^{\text{III}}(\text{bpy})$  and  $\text{M}^{\text{III}}(\text{bpy}^-)$  modes are lacking because the former are obscured by ground state scattering. In the case of  $^*\text{Os}(\text{bpy})_3^{2+}$ , the highest frequency  $\text{Os}^{\text{III}}(\text{bpy}^-)$  mode ( $1558\text{ cm}^{-1}$ ) appears at nearly the same frequency as a ground state peak ( $1559\text{ cm}^{-1}$ ) (see Figure 4). The two can be discriminated, however, by observing the intensity and peak width of the  $1558\text{--}1559\text{ cm}^{-1}$  feature as a function of laser pulse energy (compare the  $1610\text{ cm}^{-1}$  intensity to that at ca.  $1559\text{ cm}^{-1}$  in the pulsed and continuous wave spectra in Figure 4).

The  $\text{M}^{\text{III}}(\text{bpy}^-)$  frequencies of  $^*\text{Os}(\text{bpy})_3^{2+}$  average approximately  $5\text{ cm}^{-1}$  higher than those of  $^*\text{Ru}(\text{bpy})_3^{2+}$ , as can be seen by comparing the asterisked frequencies in Figure 5. In turn, the  $\text{Ru}^{\text{III}}(\text{bpy}^-)$  frequencies in  $^*\text{Ru}(\text{bpy})_3^{2+}$  average approximately  $10\text{ cm}^{-1}$  higher than those of  $\text{Li}^+(\text{bpy}^-)$ . This progression can be understood by considering the precise nature of the predominantly bpy  $\pi^*$  orbital wherein the odd electron resides in  $\text{Li}^+(\text{bpy}^-)$ ,  $^*\text{Ru}(\text{bpy})_3^{2+}$ , and  $^*\text{Os}(\text{bpy})_2^{2+}$ .

The orbital occupied by the odd electron in  $\text{Li}^+(\text{bpy}^-)$  is essentially a pure bpy  $\pi^*$  orbital, because no  $\text{Li}^+$  orbitals exist with the proper energy and symmetry to mix with the ligand  $\pi$  system. In the case of  $\text{Ru}^{2+}$  and  $\text{Os}^{2+}$ , however, metal orbitals (in octahedral symmetry, the  $t_{2g}$  set of 4d and 5d orbitals) are available which possess  $\pi$  symmetry with respect to the ligands and which have energies appropriate for mixing with the ligand  $\pi$  orbitals. The bpy orbital of interest, the lowest energy  $\pi^*$  orbital, will mix with one of these d orbitals to produce a bonding and antibonding pair. The bonding member of this pair is predominantly metal in character because the metal orbital is at lower energy than the bpy  $\pi^*$ , and the antibonding member is predominantly bpy  $\pi^*$ . It is this antibonding combination of metal d and ligand  $\pi^*$  orbitals that is the terminal orbital of MLCT excitation, and the orbital containing the odd "bpy radical" electron in the excited state. To the extent that this orbital has fractional metal character, a smaller fraction of the odd electron density is resident in the bpy  $\pi^*$  system in  $^*\text{M}(\text{bpy})_3^{2+}$  than is the case in  $\text{Li}^+(\text{bpy}^-)$ . Accordingly, the vibrational frequencies of "bpy $^-$ " in  $\text{M}^{\text{III}}(\text{bpy})_2(\text{bpy}^-)^{2+}$  are somewhat higher in both the Ru and Os systems than in  $\text{Li}^+(\text{bpy}^-)$ .

Between Ru and Os, the metal character of the predominantly bpy  $\pi^*$  orbital increases as the energy difference between the d and  $\pi^*$  orbitals decreases (i.e., as the " $t_{2g}$ " orbitals increase in energy). This energy difference is smaller in  $\text{Os}(\text{bpy})_3^{2+}$  than in  $\text{Ru}(\text{bpy})_3^{2+}$  as can be seen from the MLCT absorption maxima (Os = 490 nm; Ru = 455 nm) and the emission maxima (Os = 710 nm; Ru = 600 nm). Therefore the metal d orbital character of the "bpy  $\pi^*$ " orbitals in  $\text{M}(\text{bpy})_3^{2+}$  is greater for M = Os than for M = Ru, and the vibrational frequencies of "bpy $^-$ " are higher

in  $\text{Os}^{\text{III}}(\text{bpy})_2(\text{bpy}^-)^{2+}$  than in  $\text{Ru}^{\text{III}}(\text{bpy})_2(\text{bpy}^-)^{2+}$ .

It is clear from the foregoing discussion that the symmetry of the  $^*\text{M}(\text{bpy})_3^{2+}$  MLCT excited state which is the predominant species present between a few hundred picoseconds and ten nanoseconds after excitation (i.e., the time scale between the absorption of a photon by the ground state to produce  $^*\text{M}(\text{bpy})_3^{2+}$  and the Raman scattering of a second photon by  $^*\text{M}(\text{bpy})_3^{2+}$ ) cannot be  $D_3$ , but is at most  $C_2$  and could be lower. The TR<sup>3</sup> results do not directly prove that the emitting species does not have  $D_3$  symmetry, but only that the principal  $^*\text{M}(\text{bpy})_3^{2+}$  species does not. It is conceivable that emission could be an activated process involving only a minor fraction of the total  $^*\text{M}(\text{bpy})_3^{2+}$  at any given time. This possibility appears to be ruled out, however, by the recent fluorescence polarization results<sup>8,9</sup> which demonstrate that the emitting species has less than threefold symmetry. These conclusions regarding the symmetry of the  $^*\text{M}(\text{bpy})_3^{2+}$  state require reinterpretation of a large volume of photophysical data (ref 3, 5, 28, and references therein).

The present results demonstrate that the localized model of  $^*\text{M}(\text{bpy})_3^{2+}$  is valid on the time scales of electronic motions and molecular vibrations. It is virtually certain that delocalization (via, for example, intramolecular electron transfer or dynamic Jahn-Teller effects) occurs on some longer time scale. The present experiments are mute as to the time scale on which delocalization may occur. EPR results on  $\text{Ru}(\text{bpy})_3^{2+}$  demonstrate localization of the  $\text{bpy}^-$  electron density in this  $\text{Ru}^{\text{II}}(\text{bpy})_2(\text{bpy}^-)^+$  species on the EPR time scale,<sup>13</sup> but suggest that delocalization may occur on a time scale only slightly longer. It is possible that either time-resolved EPR or temperature-dependent fluorescence depolarization experiments, underway in these laboratories, may establish the time scale of delocalization in  $^*\text{Ru}(\text{bpy})_3^{2+}$ . Another potentially fruitful approach is to attempt to observe the bpy  $\leftarrow$   $\text{bpy}^-$  intervalence transfer absorbance which should be present in  $^*\text{Ru}(\text{bpy})_3^{2+}$ .

This study and others in this series<sup>2,10-12</sup> as well as results from other laboratories<sup>29-32</sup> clearly establish TR<sup>3</sup> as the most versatile and generally applicable probe presently available which provides direct information on the structures of electronically excited states in fluid media, the relevant conditions for essentially all photobiology as well as much photochemistry and photophysics. Such structural information is crucial (a) to test (as is the present case) conclusions on excited state parameters drawn from less structure-specific experimental probes or from theoretical approaches, (b) to establish excited state potential surfaces experimentally under chemically relevant conditions, and (c) in general to understand the mechanisms whereby light is converted into chemical energy. Our efforts to extend both the temporal range and the chemical range of applicability of TR<sup>3</sup> and related laser spectroscopies are continuing.

**Acknowledgment.** This research was supported by National Science Foundation Grants CHE 78-09338 and CHE81-09541 and Robert A. Welch Foundation Grant F-733.

(28) Paskuch, B. J.; Lacky, D. E.; Crosby, G. A. *J. Phys. Chem.* **1980**, *84*, 2061.

(29) Wilbrandt, R.; Jensen, N. H.; Pagsberg, P.; Sillesen, A. H.; Hansen, K. B. *Nature (London)* **1978**, *276*, 167.

(30) Jensen, N. H.; Wilbrandt, R.; Pagsberg, P. B.; Sillesen, A. H.; Hansen, K. P. *J. Am. Chem. Soc.* **1980**, *102*, 7441.

(31) König, R.; Lau, A.; Weigmann, H. *J. Chem. Phys. Lett.* **1980**, *69*, 87.

(32) Asano, M.; Königstein, J. A.; Nicollin, D. *J. Chem. Phys.* **1980**, *73*, 688.